

# Synthesis and Characterization of Borosilicate Glasses for Biological Applications.

Hany Kamal<sup>1\*</sup>, Dania Waggas<sup>1</sup>, Ranad Khashab<sup>1</sup>, Dalia Ramadan<sup>1</sup>,  
Rahaf Aldubaiban<sup>1</sup>

<sup>1</sup>Fakeeh College for Medical Sciences-P.O. Box 2537, Jeddah 21461 KSA.

---

## Abstract:

**Background:** Bioactive glasses are amorphous silicate-based materials compatible with the human body, bonded to bones, and capable of stimulating new bone formation while dissolving over time. They therefore have the potential to restore diseased or damaged bone to its original state and function (bone regeneration) and therefore have a myriad of applications due to their unique biological and mechanical characteristics in the fields of bone and tissue engineering. Borate is a type of bioactive glass that has been extensively investigated for biomedical applications. Boron is a vital trace element in the human body that has significant functions. It's found in the body in the form of organoboron complexes, of which 96% are boric acid and the rest are borate anion. Due to the favorable qualities of boron in tissue regeneration borate bioactive glass are processed by substituting silica ions with boron ions in the glass network.

**Objectives:** Preparation of bioactive glass material for use in medicine, measuring silicate bioglass tissue scaffolding capacity, and comparing its behavior to other bioglass currently available on the market is a key objective of this study.

**Materials and Methods:** An experimental study will be conducted to determine the preparation of borate bioactive glass and its in vitro properties for simulated body fluid, as well as document it with hydroxyapatite precipitation.

**Results:** Characterization of Borosilicate bio glass through differential scanning Calorimetry (DSC), sintering at different temperatures, glass transition temperature (T<sub>g</sub>), crystallization initiation temperature (T<sub>x</sub>), as well as FT-IR spectrum analysis. The results show changes in density, porosity, and crystallization behavior at different sintering temperatures, with the emergence of diffraction peaks indicating crystallization at higher temperatures. The FT-IR spectrum reveals characteristic vibrations of various bonds present in the glass. Immersion in simulated body fluid affects the pH levels due to leaching of Na<sup>+</sup> and Ca<sup>2+</sup>, leading to weight changes in different glass compositions. S40B10 exhibited significant weight loss at lower pH levels, emphasizing the impact of pH on the glass properties and behavior. A study on amorphous glass scaffolds revealed distinct peaks in XRD patterns when immersed in simulated body fluid (SBF). While the as-prepared glass showed a shallow peak, submerged samples exhibited a notable peak at 36°, corresponding to hydroxyapatite (HA). Analysis of S25B25 glass soaked in SBF for 7 days showed no formation of a crystalline phase, evidenced by changes in peak amplitude and the absence of certain peaks, indicating the dissolution of the scaffold without crystal formation.

**Conclusion:** Capabilities of Boron bioactive glass S25B25 as a tissue engineering scaffold were assessed. The glass exhibited antibacterial and lytic properties beneficial for bone treatment, but the focus was on creating highly porous scaffolds with interconnected pores crucial for clinical success in tissue engineering. The crystallization and sintering behavior of S25B25 were examined at temperatures ranging from 500°C to 600°C without the use of a blowing agent. Interestingly, glass S25B25 displayed a crystalline peak at 540°C. Bioactive glass scaffolds using foaming agent NH<sub>4</sub>(HCO<sub>3</sub>) were developed, and observations during sintering revealed that glass crystallization was hindered with larger glass particles, maintaining an amorphous nature at 540°C. Despite a low weight loss and moderate degradation rate, S25B25 showed rapid conversion to hydroxyapatite, indicating potential for apatite formation and successful fabrication of porous scaffolds supporting tissue ingrowth

**Key Word:** bioglass, boron, medical applications, scaffold.

---

Date of Submission: 18-03-2024

Date of Acceptance: 28-03-2024

---

## I. Introduction

Organ and tissue loss has become one the most common, problematic and costly healthcare issues encountered in modern health care. Thus, the emerging field of biomedical tissue engineering provides a

valuable solution for the replacement and regeneration of tissues and organs [1,2]. Biomaterials are naturally found or lab developed resources that are used to substitute and aid the physiology of tissues. Bioactive materials are developed to mimic the intended tissue or organ's biological structure and role [3]. Once the bioactive material is implanted it goes through a two-step reaction. During the first stage in reaction with simulated body fluid the material undergoes specific surface reactions thus during the second stage forming a hydroxyapatite layer within the tissue [4]. Hydroxyapatite is responsible for interactions within the hard & soft tissues and represents essential criteria to assess the bioactivity of a biomaterial in vivo [5].

#### **Hydroxyapatite formation and bio glass mechanism of activity:**

Bioglasses are formed of minerals (SiO<sub>2</sub>, Ca, Na<sub>2</sub>O, H, and P) naturally found in the human body; additionally, the ratios of phosphorus and calcium oxides are mimicking the same proportion in bones. Standard bioglass (45S5) formula composition according to the percentage of weight is 45% silica (SiO<sub>2</sub>), 24.5% calcium oxide (CaO), 24.5% sodium oxide (Na<sub>2</sub>O), and 6% phosphorous pentoxide (P<sub>2</sub>O<sub>5</sub>). Upon implantation to a simulated body fluid the bioglass converts to a silica-CaO/P<sub>2</sub>O<sub>5</sub>-rich gel layer that by a series of reactions mineralizes into hydroxycarbonate in a span of hours [6–8]. The resultant layer is a hydroxyapatite matrix enabling bone tissue growth and osteoblast formation [9,10]. Hydroxyapatite Ca<sub>10</sub>(PO<sub>4</sub>)<sub>6</sub>(OH)<sub>2</sub> is the natural form of calcium appetite. The bioactivity index is used to measure the bioactivity level of a potential biomaterial (IB) by calculating the duration needed for more than half of the interface to bond.

$$IB = 100/t(0.5bb)$$

In order for Biomaterials to bind to soft and hard tissues a high IB value greater than eight is required. Other Biomaterials with IB value less than 8 but more than zero will bind only to hard tissue [11]. Studies test different ratios of the minerals in the formula and certain properties of the bioglass, making it compatible for different indications in the human body accordingly [12].

#### **Types of bioactive materials**

There are four different types of generally categorized biomaterials which are natural or synthetic polymers, metals, composites, and ceramics or better known as bioglasses. While polymers are known for their flexibility allowing them unique characteristics, they are physically weak and can't demonstrate the required resistance to stress in their applications. Metals on the contrary have a high strength and wear resistance but offer low bio compatibility and with the release of metal ions. Additionally, the high number of metal ions predispose to allergic reactions and a high corrosion rate making it easily rejected by living tissues [13]. Composites have a strong composition and distinctive elastic properties but they are difficult to make and have a high production cost, they are used in the joint implants and heart valves. Ceramics are biocompatible, they are strong and resistant to compression and corrosion but unfortunately these materials are brittle, have weak tension and can often be fragile [13].

#### **Borate bioactive glass**

A Significant number of studies have shown that borate bioglasses are active [9,14]. borate bioactive glass as formed by replacing the silica ions in the classic composition with boron. Borate glasses demonstrate high reactivity as borate transforms faster than silica [14,15]. Additionally, Boron is an important element found within the human body in organ boron complexes. It is optimal to intake 1 mg of boron daily for essential body functioning [16–18]. boron has shown to have many therapeutic effects in the body, bone, hair, and nails as they have the highest concentration of boron [17]. Furthermore, it has been reported that the presence of boron in the body alleviates symptoms of osteoporosis, coronary heart disease, and arthritis due to its roles of improving calcium integration into bone, joints, and cartilage [19]. Due to these properties Boron bioactive glasses are formulated into specific compositions to achieve osteoconductivity, biodegradability whilst being bioactive, surpassing the performance of silicate Bioglasses when used for bone regeneration, wound healing, and nerve tissue engineering applications [20].

The aim of this paper is to prepare a bioactive glass material to be used in the medical field. This experimental study will focus on formulating a borate bioactive glass and test its in vitro properties in simulated body fluid and document its hydroxyapatite precipitation. The paper will furthermore measure boro-silicate bioglass tissue scaffolding capacity and compare its behavior to other bioglasses currently available in the market.

## **II. Material And Methods**

All materials used in the preparation of the borosilicate bioglass with scaffolds are attached in table 1 with the respective ratio in composition.

**Table 1: Composition of S25B25 presented in (Mol. %)**

Glass name	Chemical composition
S25B25	25SiO <sub>2</sub> -25B <sub>2</sub> O <sub>3</sub> -24Na <sub>2</sub> O-20CaO-6P <sub>2</sub> O <sub>5</sub>

### Procedure methodology

The starting materials for the Boron bioglass S25B25 were analytical reagent grades: Na<sub>2</sub>CO<sub>3</sub>, H<sub>3</sub>BO<sub>3</sub>, CaCO<sub>3</sub>, CaHPO<sub>4</sub>·2H<sub>2</sub>O and 99.4 percent pure SiO<sub>2</sub> respectively. Making the resultant composition of the Glass S25B25 a composition of 40SiO<sub>2</sub>-10B<sub>2</sub>O<sub>3</sub>-24Na<sub>2</sub>O- 20CaO-6P<sub>2</sub>O<sub>5</sub>.The powder mixture made from the starting material was made in aluminum crucibles and melted at 1100 degree Celsius for one hour for the borate bioglass S25B25.

The crushed powders were packed in a tungsten carbide grinding bowl (76 mm) and milled in a planetary ball mill. A 3 wt% additive was added for PEG (polyethylene glycol) and Dolapix C64. After milling, the powder was dried in the oven at 70°C for 24 hrs. The material formed during the drying process was granulated using a porcelain mortar and pestle. The powders were then moved through a stainless-steel sieve of 100 μm using a sieve shaker. The NH<sub>4</sub>(HCO<sub>3</sub>) foaming agent and the glass powder mixtures were prepared by mixing 2 grams which were rotated at a speed of 96 rpm for 30 minutes where 12 aluminum milling balls (2 mm). The foaming agent ammonium bicarbonate NH<sub>4</sub>(HCO<sub>3</sub>) was applied with a material of 70 vol.%. To establish porous bioactive glass scaffolds, samples were sintered with and without the foaming agent ammonium bicarbonate NH<sub>4</sub>(HCO<sub>3</sub>) respectively. Samples with ammonium bicarbonate NH<sub>4</sub>(HCO<sub>3</sub>) were sintered for 1 hour at 540 °C for S25B25 and 500 °C after burning with NH<sub>4</sub>(HCO<sub>3</sub>) foaming agent at 65 °C for 2 hours. Scaffolds were treated and immersed in simulated body fluid (SBF) solution at 37°C as suggested by Kokubo et al. [4-5].

## III. Result And Discussion

### Thermal Properties of Glasses

The term "thermal property" refers to a material's reaction to heat application. A solid's dimensions may expand and the absorbed heat energy may move from a temperature-higher zone to a temperature-lower region in accordance with the temperature gradient as its temperature rises as a result of heat absorption, eventually melting the specimen. When using glass for applications, its thermal conductivity, thermal shock resistance, thermal expansion resistance, and transistor heat capacity are frequently taken into account [21].

The glass transition temperature (T<sub>g</sub>) and crystallization initiation temperature (T<sub>x</sub>) of the glasses were estimated using a differential scanning Calorimetry (DSC). The DSC traces of the glasses are captured on powder samples with a particle size range of 100–300 m at a heating rate of 10 °C/min (Fig. 1). DSC traces of S25B25 exhibit an endothermic effect at T<sub>g</sub> glass transition temperature, or the endotherm inflection point, which is around 540 °C. This is followed by T<sub>x</sub> crystallization start temperature, or the endothermic and exothermic peak inflection points, which is 630 °C[22,23].

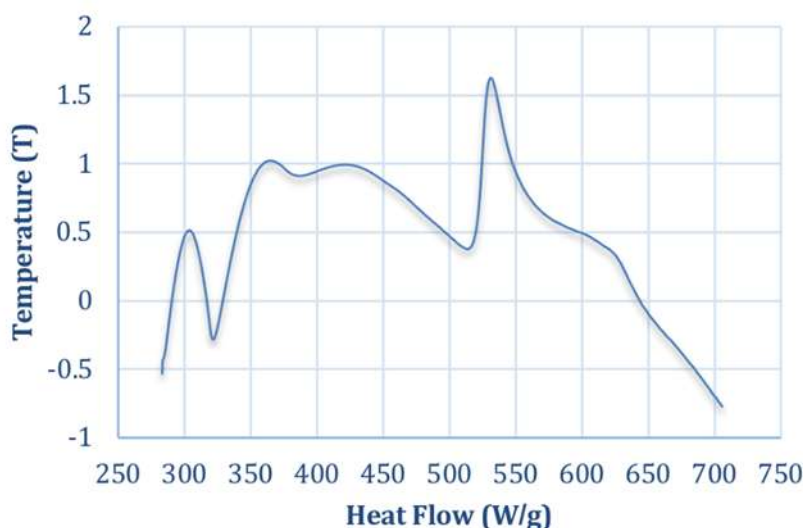


**Figure 1:** DSC thermographs of the glasses of investigation

Figure 2 illustrates SEM for glass sample powder that was made with NH<sub>4</sub>(HCO<sub>3</sub>). We can see a pattern where the amorphous and post-milling phases (i.e., amorphous) frequently displayed varied uneven

forms with a broad distribution scale. If we compare the force utilized during crushing to the force used for destroying glasses that are prepared without  $\text{NH}_4(\text{HCO}_3)$ , the high particle size obtained for the glasses prepared with  $\text{NH}_4(\text{HCO}_3)$  was the consequence of the lower force used during crushing. This particle size increase was essential for enhancing the crystallization of bioactive glass powders because fine particles have been described [22–25].

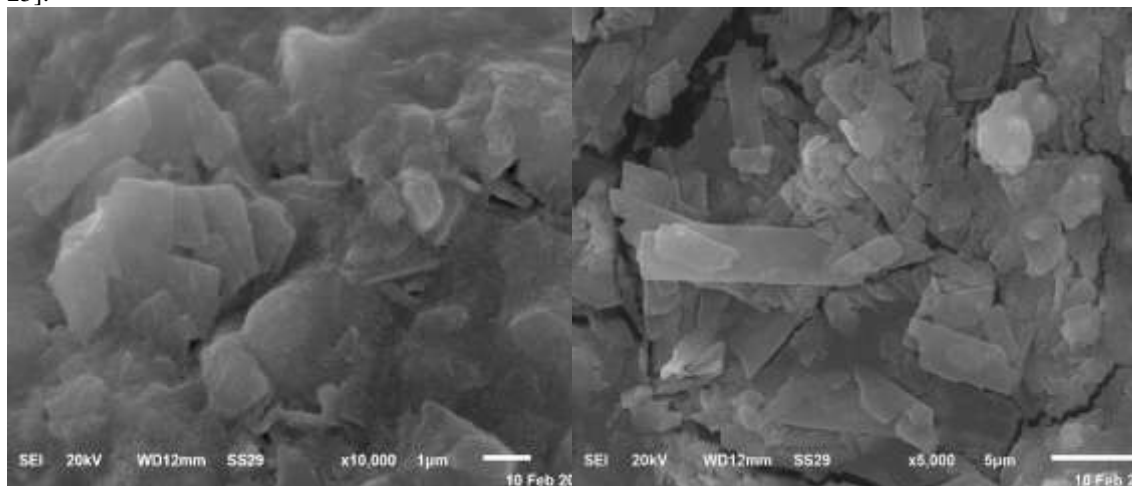


**Figure 2:** SEM images of S25B25 powder showing the particle size and shape prepared

### Characterization of Borate Bioactive Glasses for Medical Applications

#### Sintering of Glass Powder

The glass samples were sintered without the foaming agent in order to identify the appropriate sintering conditions that would be used to create porous glass scaffolds while also assessing the sintering behavior of the glasses.

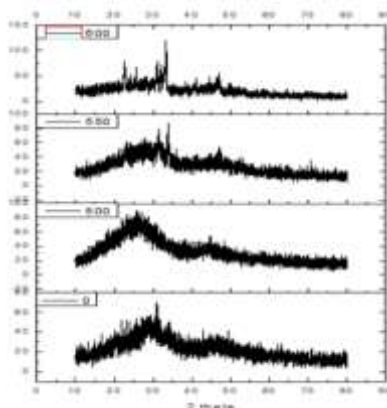
The obtained densities of sintered bioactive glasses are shown in Table 2 and Figure 3. When the temperature raised further, it was seen that the density increased to a certain point and then decreased to 600 °C. This indicates that densification is impeded at high sintering temperatures. Porosity behaves in a manner that is contrary to density [3,10–12].

**Table 2: Composite, Temperature during sintering, Density, Relative density, and Porosity**

Composite	Si25B25		
Sintering temperature	500 °C	550 °C	600 °C
Density ( $\text{g}/\text{cm}^3$ )	2.16±0.02	2.48±0.02	2.25±0.02
Relative Density (%)	86	92	86
Porosity (%)	18±0.12	12±0.22	14±0.32

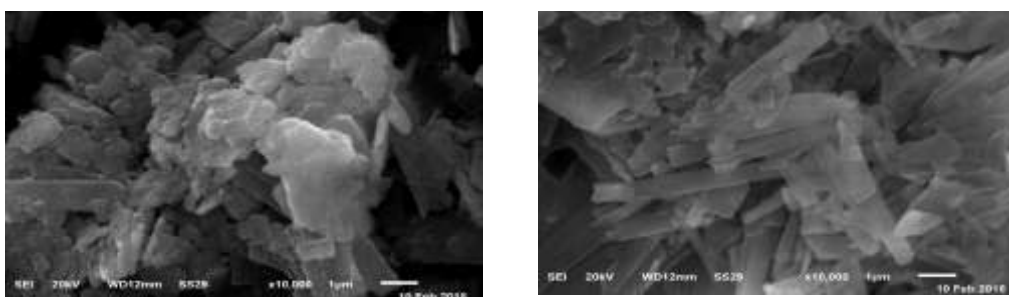
As shown by the previous table the Borosilicate bio glass was sintered at 500,550, and 600 degrees Celsius. At 500 degrees Celsius the density of the composite was 2.16±0.02 ( $\text{g}/\text{cm}^3$ ) with the relative density being 86% and its porosity 18%±0.12. At 550°C the borosilicate bio glass had the highest recorded density of 2.48±0.02 ( $\text{g}/\text{cm}^3$ ) with the lowest porosity finding of 12% ±0.02 and the relative density at a maximum of 92%. At the highest temperature of 600°C the density is recorded at 2.25±0.02 ( $\text{g}/\text{cm}^3$ ), the porosity 14%±0.32 and a recurring relative density of 86%.

Figure 3. Shows XRD patterns for the bioactive glasses at each sintering temperature for S25B25. The XRD measurements revealed that glass S25B25 had a similar behavior in maintaining an amorphous structure at 550 °C for sintering. However, when the sintering temperature increased, all the glasses started to crystallize, as seen by the emergence of strong diffraction peaks with a noticeable degree of crystallization at 600 °C.



**Figure 3.** XRD pattern for glass S25B25 as a function of temperature

The samples were further characterized using SEM to examine their microstructure after sintering. Analysis of the microstructure during sintering shows formation of hydroxyapatite clusters which upon coalescence by heat alter to spindle shape with needle-like projections.



**Figure 4.** SEM of S25B25 microstructure during sintering

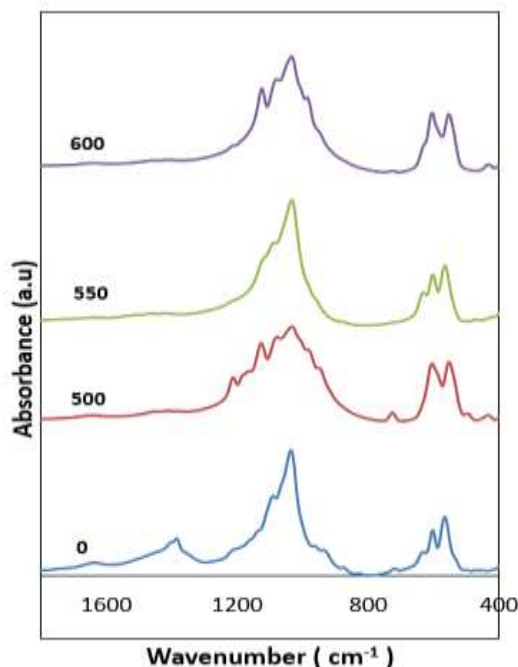


**Figure 5.** FTIR spectrum of S25B25

FTIR spectrum of the borosilicate glass was conducted as seen by figure 5. The peak at approximately  $1402\text{ cm}^{-1}$  is ascribed to symmetric stretching relaxation of the B-O band of trigonal  $\text{BO}_3$  units [37]. The broad absorption band observed at approximately  $1095\text{ cm}^{-1}$  can be assigned to tri-, tetra-, pentaborate and diborate groups belonging to  $\text{BO}_3$  and  $\text{BO}_4$  groups along with asymmetric stretching Si-O-Si bonds. The band at  $925\text{ cm}^{-1}$  should be assigned to the B-O vibration of  $\text{BO}_4$  units and is also associated with the stretching frequency of Si\O\B [38]. The bond at approximately  $800\text{ cm}^{-1}$  is assigned to the symmetric stretching vibration of O-Si-

O. The band at  $680\text{ cm}^{-1}$  is assigned to the bending vibration of bridging oxygen (B-O) between trigonal  $\text{BO}_3$  groups. A broad band centered at  $450\text{ cm}^{-1}$  corresponds to the Si-O-Si bending vibration [26].

### **In Vitro Properties**

#### **Variation of pH**

The tubes were immersed in simulated body fluid (SBF) for 1, 2, 3, and 7 days. pH of SBF at room temperature is 7.4. The pH was seen to increase with the longer S25B25 immersion time with a maximum pH of 26 at 7 days. Additionally, the pH levels of the scaffold are 70 vol. The leaching of  $\text{Na}^+$  and  $\text{Ca}^{2+}$  into the solution and the concurrent formation of a layer rich in  $\text{SiO}_2$  were the causes of the rise in pH, which resulted in a simpler pH [3,10,14,23,26].

**Variation of mass:** The change in mass was also measured to determine how much weight was lost through immersion. The conversion and dissolution reactions that caused the scaffolds to lose weight when immersed in SBF solution are the same as the reactions that regulate the pH of solution, so weight loss and the pH results are expected to follow approximately the same trends. [3,10,14,23,26].

The adjustment of the weight of S40B10 is shown in Fig.6 It is important to note that S40B10 continued to gain weight steadily after the initial dramatic increase. Lower pH levels resulted in a high percentage of weight loss for S40B10.

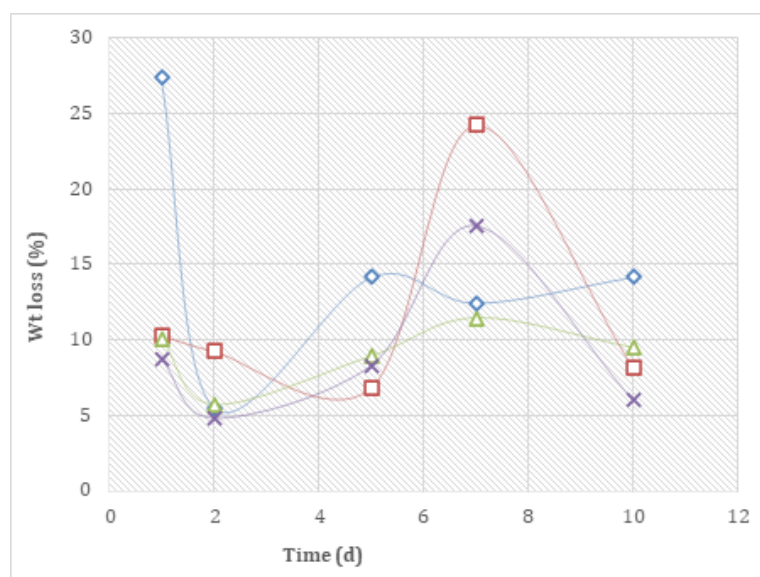


**Figure 6. Weight loss of scaffold throughout immersion in SBF solution**

### **Phase and Microstructural analysis:**

#### **XRD analysis:**

A common characteristic of any amorphous glass composition was the frequently seen shallow big peak on the as-prepared glass scaffold. Conversely, the submerged samples' XRD patterns showed a notable peak at  $36^\circ$ , which was consistent with the HA peak.

These results suggest that SBF dissolves the scaffolds and causes  $\text{Ca}_4\text{O}(\text{PO}_4)_2$  to produce a weak crystalline phase. By employing Cu K5-007, this peak is normally placed at about  $32^\circ$ ; however, in this case, the peak location may have changed due to the usage of Co K5-007 [27-28]. As the porosity and immersion time rose, so did the intensity of both peaks. Nevertheless, the peak intensities remained significantly lower than those of the conventional crystalline HA, indicating that the as-prepared [29–31].

Phase analysis of S25B25 glass was performed only on scaffolds soaked in SBF for 7 days. XRD was selected after 7 days to determine only the formation of the HA layer. The XRD pattern of S25B25 soaked for 7 days remained the same as the untreated glass. This indicates that SBF dissolves the skeleton without forming a crystalline phase. This is evident from the decrease in peak amplitude, the development of new peaks, and the absence of certain peaks [32].

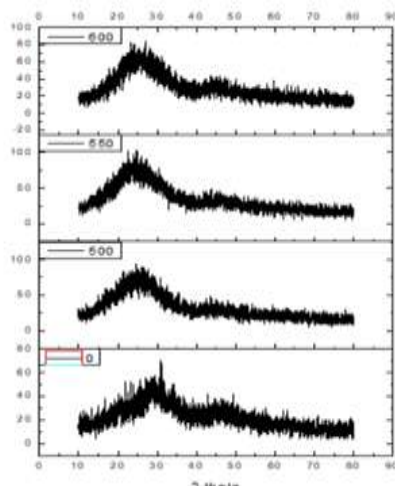


Figure 7. XRD for samples soaked in SBF at different time intervals

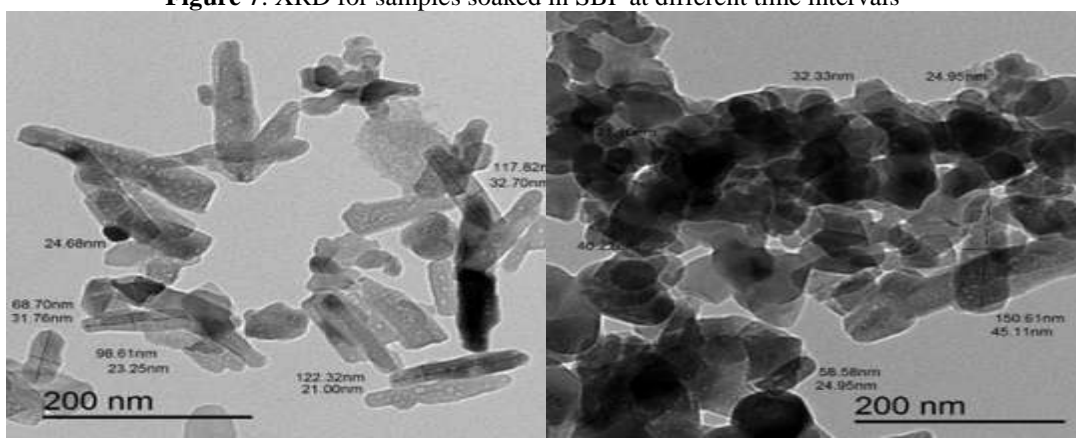


Figure 8. SEM analysis of dimensions of microstructure during sintering

SEM analysis of the dimensions show an average width of 26.678 nm and length of 101.862 nm before sintering and after sintering a width of 33.11 nm and height of 104.59nm.

#### IV. Conclusion

In this article, we measured the capabilities of a Boron bioactive glass (S25B25) tissue engineering scaffold. In the past, these glasses were found to have antibacterial and lytic properties that are promising for the treatment of damaged bone. However, it is well known that tissue engineering requires scaffolds with high porosity and interconnected pores to achieve optimal clinical applications. The crystallization and sintering ability of S25B25 was examined at temperatures between 500°C and 600°C without the addition of blowing agent  $\text{NH}_4(\text{HCO}_3)$ . Glass S25B25 showed a crystalline peak at 540 °C.

Bioactive glass scaffolds with these formulations (S25B25) were developed using foaming agent ( $\text{NH}_4(\text{HCO}_3)$ ) at a content of 70 vol%. For glass samples, rates with sintering at 550 °C for 1 h at a heating rate of 10 °C/min. As observed during sintering, we found that glass crystallization was suppressed to some extent by increasing the size of the glass particles. No crystallization peak was observed at 540 °C for S25B25 compared to the sample sintered without ammonium bicarbonate.  $\text{NH}_4(\text{HCO}_3)$  This suggests that the framework of these two compositions retains amorphous nature.

Despite the low weight loss and moderate degradation rate of S25B25 was found to have the fastest conversion rate to HA. These glass compositions have shown promise in terms of apatite formation, and porous scaffolds can be successfully fabricated while retaining their amorphous nature, which supports tissue ingrowth. It is advantageous to do so.

#### References

- [1] R.M. Nerem, Cellular Engineering, Ann Biomed Eng 19 (1991) 529–545. <https://doi.org/10.1007/Bf02367396>.
- [2] J.P. Vacanti, R. Langer, Tissue Engineering: The Design And Fabrication Of Living Replacement Devices For Surgical Reconstruction And Transplantation, Lancet 354 (1999) 32–34. [https://doi.org/10.1016/S0140-6736\(99\)90247-7](https://doi.org/10.1016/S0140-6736(99)90247-7).
- [3] L.G. Donaruma, Definitions In Biomaterials, D. F. Williams, Ed., Elsevier, Amsterdam, 1987, 72 Pp., Journal Of Polymer Science Part C: Polymer Letters 26 (1988) 414–414. <https://doi.org/10.1002/Pol.1988.140260910>.

- [4] T. Kokubo, H. Takadama, How Useful Is Sbf In Predicting In Vivo Bone Bioactivity, *Biomaterials* 27 (2006) 2907–2915. <https://doi.org/10.1016/j.biomaterials.2006.01.017>.
- [5] T. Kokubo, H. Kushitani, S. Sakka, T. Kitsugi, T. Yamamuro, Solutions Able To Reproduce In Vivo Surface-Structure Changes In Bioactive Glass-Ceramic A-W3, *J Biomed Mater Res* 24 (1990) 721–734. <https://doi.org/10.1002/jbm.820240607>.
- [6] H. Andersson, I. Kangasniemi, Calcium Phosphate Formation At The Surface Of Bioactive Glass In Vitro, *J Biomed Mater Res* 25 (1991) 1019–1030. <https://doi.org/10.1002/jbm.820250808>.
- [7] L.L. Hench, J. Wilson, Surface-Active Biomaterials, *Science* 226 (1984) 630–636. <https://doi.org/10.1126/science.6093253>.
- [8] K.E. Wallace, R.G. Hill, J.T. Pembroke, C.J. Brown, P. V. Hatton, Influence Of Sodium Oxide Content On Bioactive Glass Properties, *J Mater Sci Mater Med* 10 (1999) 697–701. <https://doi.org/10.1023/A:1008910718446>.
- [9] P. Ducheyne, Q. Qiu, Bioactive Ceramics: The Effect Of Surface Reactivity On Bone Formation And Bone Cell Function, *Biomaterials* 20 (1999) 2287–2303. [https://doi.org/10.1016/S0142-9612\(99\)00181-7](https://doi.org/10.1016/S0142-9612(99)00181-7).
- [10] Developments In Biocompatible Glass Compositions, (N.D.). <https://www.mddionline.com/medical-device-markets/developments-in-biocompatible-glass-compositions> (Accessed January 14, 2024).
- [11] L.L. Hench, *Bioceramics: From Concept To Clinic*, (N.D.).
- [12] Cerruti, M., Greenspan, D., & Powers, K. (2005). Effect Of Ph And Ionic Strength On The Reactivity Of Bioglass® 45s5. *Biomaterials*, 26(14), 1665-1674.
- [13] K. Yang, Y. Ren, Nickel-Free Austenitic Stainless Steels For Medical Applications, *Sci Technol Adv Mater* 11 (2010) 014105. <https://doi.org/10.1088/1468-6996/11/1/014105>.
- [14] A. Yao, D. Wang, W. Huang, Q. Fu, M.N. Rahaman, D.E. Day, In Vitro Bioactive Characteristics Of Borate-Based Glasses With Controllable Degradation Behavior, *Journal Of The American Ceramic Society* 90 (2007) 303–306. <https://doi.org/10.1111/j.1551-2916.2006.01358.x>.
- [15] W. Huang, D.E. Day, K. Kittiratanapiboon, M.N. Rahaman, Kinetics And Mechanisms Of The Conversion Of Silicate (45s5), Borate, And Borosilicate Glasses To Hydroxyapatite In Dilute Phosphate Solutions, *J Mater Sci Mater Med* 17 (2006) 583–596. <https://doi.org/10.1007/S10856-006-9220-Z>.
- [16] D. Ege, K. Zheng, A.R. Boccaccini, Borate Bioactive Glasses (Bbg): Bone Regeneration, Wound Healing Applications, And Future Directions, *Acs Appl Bio Mater* 5 (2022) 3608. <https://doi.org/10.1021/acsbm.2c00384>.
- [17] Ö.E. Akdere, İ. Shikhaliyeva, M. Gümüşderelioğlu, Boron Mediated 2d And 3d Cultures Of Adipose Derived Mesenchymal Stem Cells, *Cytotechnology* 71 (2019) 611. <https://doi.org/10.1007/S10616-019-00310-9>.
- [18] A. Biță, I.R. Scorei, T.A. Bălșeanu, M.V. Ciocilteu, C. Bejenaru, A. Radu, L.E. Bejenaru, G. Rău, G.D. Mogoșanu, J. Neamțu, S.A. Benner, New Insights Into Boron Essentiality In Humans And Animals, *Int J Mol Sci* 23 (2022). <https://doi.org/10.3390/ijms23169147/S1>.
- [19] L. Pizzorno, Nothing Boring About Boron, *Integrative Medicine: A Clinician's Journal* 14 (2015) 35. <https://www.ncbi.nlm.nih.gov/pmc/articles/PMC4712861/> (Accessed January 14, 2024).
- [20] D. Ege, K. Zheng, A.R. Boccaccini, Borate Bioactive Glasses (Bbg): Bone Regeneration, Wound Healing Applications, And Future Directions, *Acs Appl Bio Mater* 5 (2022) 3608–3622. [https://doi.org/10.1021/acsbm.2c00384/asset/images/large/mt2c00384\\_0011.jpeg](https://doi.org/10.1021/acsbm.2c00384/asset/images/large/mt2c00384_0011.jpeg).
- [21] J. Galbraith, L. Chapman, J.W. Zwanziger, M. Aldridge, J. Kieffer, Elasto-Optic Coefficients Of Borate, Phosphate, And Silicate Glasses: Determination By Brillouin Spectroscopy, *The Journal Of Physical Chemistry C* 120 (2016) 21802–21810. <https://doi.org/10.1021/acs.jpcc.6b07202>.
- [22] J. Will, L.C. Gerhardt, A.R. Boccaccini, Bioactive Glass-Based Scaffolds For Bone Tissue Engineering., *Adv Biochem Eng Biotechnol* 126 (2012) 195–226. [https://doi.org/10.1007/10\\_2011\\_106/Cover](https://doi.org/10.1007/10_2011_106/Cover).
- [23] Q. Liu, J. Wang, T. Xiu, Fabrication And Characterization Of Mesoporous Borosilicate Glasses With Different Boron Contents, *J Mater Res* 22 (2007) 1834–1838. <https://doi.org/10.1557/Jmr.2007.0251>.
- [24] A.H. Yao, D.P. Wang, Q. Fu, W.H. Huang, M.N. Rahaman, Preparation Of Bioactive Glasses With Controllable Degradation Behavior And Their Bioactive Characterization, *Chinese Science Bulletin* 52 (2007) 272–276. <https://doi.org/10.1007/S11434-007-0023-5/Metrics>.
- [25] A. Yao, D. Wang, W. Huang, Q. Fu, M.N. Rahaman, D.E. Day, In Vitro Bioactive Characteristics Of Borate-Based Glasses With Controllable Degradation Behavior, *Journal Of The American Ceramic Society* 90 (2007) 303–306. <https://doi.org/10.1111/j.1551-2916.2006.01358.x>.
- [26] P.W. Anderson, B.I. Halperin, C.M. Varma, Anomalous Low-Temperature Thermal Properties Of Glasses And Spin Glasses, *Philosophical Magazine* 25 (1972) 1–9. <https://doi.org/10.1080/14786437208229210>.
- [27] Rizwan, M., Hamdi, M., & Basirun, W. J. (2017). Bioglass® 45s5- Based Composites For Bone Tissue Engineering And Functional Applications. *Journal Of Biomedical Materials Research Part A*, 105(11), 3197-3223.
- [28] J.R. Jones, S. Lin, S. Yue, P.D. Lee, J. V. Hanna, M.E. Smith, R.J. Newport, Bioactive Glass Scaffolds For Bone Regeneration And Their Hierarchical Characterization, [http://dx.doi.org/10.1243/09544119jeim836\\_224](http://dx.doi.org/10.1243/09544119jeim836_224) (2010) 1373–1387. <https://doi.org/10.1243/09544119jeim836>.
- [29] A. Yao, D. Wang, W. Huang, Q. Fu, M.N. Rahaman, D.E. Day, In Vitro Bioactive Characteristics Of Borate- Based Glasses With Controllable Degradation Behavior, *Journal Of The American Ceramic Society* 90 (2007) 303–306.
- [30] H. Kamal, Characterization Of Silver-Borate Glasses For Biomedical Applications, *Iosr-Jap* 11 (2019) 18–26.
- [31] H. Kamal, A.M. Hezma, Structure And Physical Properties Of Borosilicate As Potential Bioactive Glasses, *Silicon* 10 (2018) 851–858. <https://doi.org/10.1007/S12633-016-9540-7>.
- [32] H. Kamal, A.M. Hezma, Spectroscopic Investigation And Magnetic Study Of Iron, Manganese, Copper And Cobalt-Doped Hydroxyapatite Nanopowders, *Phys. Sci. Int. J* 7 (2015) 137–151.